RSC Advances

PAPER

View Article Online
View Journal | View Issue

Cite this: *RSC Adv.*, 2024, **14**, 26183

Synthesis and characterization of new electrospun medical scaffold-based modified cellulose nanofiber and bioactive natural propolis for potential wound dressing applications

Yassine El-Ghoul, *[ab] Abdulmohsen S. Altuwayjiri[a] and Ghadah A. Alharbi[a]

Recently, the design of polymer nanofibers using the electrospinning process has attracted much interest. Particularly the use of natural polymers has promoted many advantages in their biomedical applications. However, the combination of multiple natural polymers remains a great challenge in terms of electrospun production and applied performance. From this perspective, the current investigation highlights the study of the preparation of electrospun nanomaterial scaffolds based on combined natural polymers for improved wound healing performance. First, we have synthesized a crosslinked polymer by reacting microcrystalline cellulose (MC) and chitosan (CS) biopolymer *via* the intermediate of citric acid as a crosslinking agent. Then a natural propolis biomolecule was incorporated into the polymer network. Different MC/CS blend ratios of 90/10 and 70/30 were then used and various machine parameters were optimized to obtain nanofiber scaffolds with excellent strength and structures. SEM, IR, physicochemical, mechanical, and morpho-logical characterization were then performed. SEM evaluation revealed homogeneous and bead-free nanofibrous structures, with well-defined morphology and a random deposition that could accurately mimic the extracellular matrix of native skin. The calculated average nanofiber diameters for the MC/CS blend ratios at 90/10 and 70/30 were 431.4 and 441.2 nm, respectively. The results showed that when the chitosan amount increased, larger nanofibers with narrow diameter distribution appeared. The prepared nanomaterials had a significant and close water vapor permeability of about 1735.12 and 1698.52 g per m per day for the two blend ratios of 90/10 and 70/30, respectively. The examination of swelling behavior revealed a noteworthy enhancement in hydrophilicity, a necessary attribute for improved healing efficacy. FT-IR analysis confirmed the success and the stability of the chemical crosslinking reaction between the two biopolymers before nanofiber conception. Excellent mechanical properties were acquired, based on the chitosan content. Both developed nanofiber scaffolds exhibited high tensile strength and Young's modulus values. The incorporation of 30% chitosan *versus* 10% results in an increase in tensile strength of 11% and 14% in Young's modulus. Therefore, we could adjust the different mechanical properties simply by varying the mixing rate of the electrospun polymers. Using epithelial HepG2 cells, viability and kinetic cell adhesion assays were assessed to obtain biological evaluation. No cytotoxicity was observed and good cytocompatibility was confirmed. Functionalized nanofiber biomaterials with different MC/CS ratios substantiated significant bactericidal effectiveness against Gram-positive and Gram-negative bacterial culture strains. The novel functional electrospun wound dressing scaffold demonstrated effective and promising biomedical performance, healing both acute and chronic wounds.

Received 9th June 2024
Accepted 14th August 2024

DOI: 10.1039/d4ra04231j

rsc.li/rsc-advances

1 Introduction

A suitable biomaterial must meet technical and biological criteria, as it comes into contact with physiological fluids and tissues over prolonged periods.[1,2] To achieve these objectives, they require high biocompatibility, or the capacity to maintain biofunctionality without having detrimental effects.[3,4] Since nanostructured materials exhibit distinctive and unique qualities, including high specific surface area and significant porosity, the specific needs of these biomaterials have stimulated researchers' interest in using nanotechnology as a viable solution to existing difficulties.[5,6] Therefore, these requirements directly affect the functionality and design of scaffolds applied

[a]*Department of Chemistry, College of Science, Qassim University, Buraidah 51452, Saudi Arabia. E-mail: y.elghoul@qu.edu.sa; 421100077@qu.edu.sa; 431214197@qu.edu.sa*

[b]*Textile Engineering Laboratory, University of Monastir, Monastir 5019, Tunisia*

in the bio-medical sector.[7,8] Over the past decade, the use of nanotechnology in medicine for various biomedical applications has gained popularity, opening new possibilities for the interaction between materials and biological systems at the nanoscale. In this regard, nano-particles are used both to trigger immune responses and to carry drugs for cancer treatment.[9–12] Conversely, nanofibers may find applications in tissue regeneration scaffolds, vascular grafts, wound dressings, and other applications.[13–15] The emergence of nano-technology and biomaterial processing methods has resulted in significant advancements in the design and construction of artificial extracellular matrices, also referred to as scaffolds.[16–18] Specifically, electrospinning is the most widely used technology for producing porous scaffolds since it is a flexible approach.[19–21] Additionally, electrospun nanofibers exhibit several interesting characteristics, including a high surface area-to-volume ratio. The diameter and shape of the resultant nanofibers can be influenced by the key adjustable operating parameters of electrospinning, which include the solution, process, and environmental factors.[22–24] By carefully regulating these factors, we can create electrospun nanomaterials with the ideal physical characteristics for advanced uses. Nanofibrous scaffolds with a variety of structural characteristics have been designed using numerous synthetic and natural biopolymers.[25–28] For synthetic polymers, the most commonly used for bone tissue engineering, heart grafts, wound dressing, and heart vessel replacement are biodegradable polymers including polylactic acid (PLA), poly-caprolactone (PCL), polyglycolic acid (PGA), polyurethane (PU), copolymer poly(lac-tic-*co*-glycolide) (PLGA), and copolymer of poly(L-lactide-*co*-ε-caprolactone) (PLLA-CL). Their mechanical qualities (viscoelasticity and strength) and faster rate of degradation allowed them to display additional advantages over natural polymers.[29–34]

In general, synthetic polymers are more affordable than natural ones and offer greater versatility in synthesis, processing, and modification. Crucially, it is possible to efficiently and selectively adjust their mechanical characteristics.[35,36] However, because synthetic polymers are not bioactive, they require more modifications than natural polymers. Additionally, due to their essentially inert nature, it remains difficult to tune the surface properties of synthetic polymers, such as wettability, hydrophilicity, and cell adhesion. It is crucial to modify the surface of nanofibers following electrospinning to improve their suitability for tissue engineering.[37,38] However, this modification is generally expensive and not always stable and could alter the original properties of the functionalized nanofibers. Conversely, scaffolds made of natural polymers promote greater cell adhesion, proliferation, and differentiation than those made of synthetic polymers because natural polymers are intrinsically bioactive and have cell-interactive domains on their backbones.[39–43] Among the natural polymers prepared by the electrospinning technique, we find collagen, nucleic acids (DNA), polysaccharides (Alginate, chitosan, hyaluronic acid chitin), and lipids (lecithin), gelatin, elastin, casein, silk fibroin, cellulose acetate, fibrinogen, *etc.*[44–55] Generally, Scaffolds based on natural polymers demonstrate better clinical performance. To further improve the efficiency of the made nanofibers, composite polymers, and co-polymers were exploited by mixing the natural and synthetic polymers in the electrospinning. Indeed, natural polymers including chitosan, gelatin, and collagen were frequently combined with synthetic polymers.[56,57] *In vivo*, studies of composite nanofibers made of synthetic and natural polymers have also been conducted. For vascular tissue engineering, for instance, electrospun composite collagen/PCL nanofibers have been studied.[58] Additionally, by blending PCL with polyethylene glycol (PEG) polymers, nanofibrous scaffolds with the right porosity for cell infiltration and growth were created.[59] Additional electrospun nanofiber scaffold combinations were created and assessed. These involved blending synthetic polymers with various bioactive inorganic minerals, such as hydroxyapatite (HA) and calcium phosphate. Promising outcomes were observed in the *in vivo* and *in vitro* cell proliferation and differentiation.[60,61]

Recently, much attention has been paid to effective bioactive biomaterials and dressings-based biopolymers in the medical field especially, to treat acute and chronic wounds.[62–67] Due to their close resemblance to the extracellular matrix (ECM) for wound healing and skin regeneration, their strong barrier qualities against external pathogens, their high porosity and permeability to air and water, electrospun nanomaterials have proven to be an excellent alternative. Indeed, electrospinning nanofiber membranes' porosity structure can imitate the natural extracellular matrix (ECM) of tissues, promoting the adhesion, migration, proliferation, and differentiation of epithelial cells.[68–70] Owing to their increased specific surface area, nanofibers may be able to perform many functions, such as halting bleeding, loading and releasing medicines more easily, and effectively absorbing exudate from traumatized areas.[71] Moreover, the substantial porosity of 60–90% of the electrospun nanofiber materials and their random mesh arrangement promote cellular respiration, limit excessive water loss, and keep the trauma surface moist. They also inhibit external microbial invasion and stop granulation tissue from growing into the dressing.[72] In light of these benefits, electrospun nanofibers have the potential to be the most promising wound dressing.

In line with this, we tried in this study to design and characterize a novel electrospun nanofibrous material based on crosslinked microcrystalline cellulose and chitosan biopolymers loaded with propolis natural biomolecule, with application in wound healing. The novelty in our investigation is summed up in the electrospinning of natural polysaccharides after their crosslinking to bring them more morphological and mechanical properties. After optimizing the electrospinning process, chemical, physicochemical, morphological, and mechanical characterizations were performed using FT-IR, swelling, contact angle, water vapor permeability, SEM, and mechanical tensile analyses. The biocompatibility of the produced nanomaterials was evaluated using XTT, glutathione (GSH), and fluorescence microscopy *in vitro* biological assays. Finally, antimicrobial tests were assessed *via* standardized microbiological procedures.

2 Materials and experimental methods

2.1. Materials

Microcrystalline cellulose white powder (MC, particle size = 51 μm), chitosan polymer (CS, with an Mw of 190 kDa and a DD of 75–85), sodium dihydrogen hypophosphite (SHP catalyst), and citric acid (the crosslinking polycarboxylic agent) were purchased from Aldrich Chemicals. All chemicals were explored as provided, without any additional modifications. White propolis powder was collected in 2022 in the northern region of Tunisia. After grinding in a mortar and freezing in liquid nitrogen, the raw propolis samples were preserved in sealed plastic bags at temperatures below −20 °C.

2.2. Viscosity assessment

Before the electrospinning procedure, the different viscosities of the polymer solutions prepared and proportioned to different concentrations were measured using a Discovery HR30 hybrid rheometer (TA Instruments New Castle, USA). The temperature was set at 25 °C, while the rate of shear was raised linearly from 10 to 100 s^{-1}.

2.3. FTIR-ATR analysis

Chemical conformational characterization of the crosslinking reaction of the synthesized polymer and the nanofibrous material was performed using an FTIR spectroscopy analysis *via* ATR mode. An FTIR spectrometer from Agilent Technologies (Gladi-ATR, CA, USA) was used. The measurements of the various spectra ranged from 4000 to 400 cm^{-1}.

2.4. SEM morphological analysis

JEOL brand SEM microscopy (JSM-5400 LV, Akishima, Japan) was used to study the surface morphological behavior of the different nanofiber materials produced. Micro-graphs were captured at a 5 kV acceleration voltage. The range of the magnification scale was 100 to 3000×. Before SEM examination, a thin layer of platinum was applied to each of the samples to increase the surface conductivity and produce images with greater resolution. Using ImageJ software, 100 separate fibers were randomly measured to determine the average nanofiber diameter, which was then displayed as "mean ± standard deviation".

2.5. Wettability and swelling capacity

Wettability and surface damping characteristics of the designed nanomaterial were assessed by the study of their ability to absorb water (surface tension 72.6 mJ m^{-2}) and glycerol (surface tension 63.4 mJ m^{-2}) as solvent tests. This was done in accordance with the ASTM D5725-99 standardized test and using the drop contact angle method with a Digidrop device. Zero seconds after placing a droplet of 5 μl on the nanomaterial's surface at 37 °C, the measurements were taken for water and glycerol respectively. Each value was determined using the following formula, which considered the mean of ten measurements:

$$\theta = 2\mathrm{Arctg}\left[\frac{2h}{D}\right] \quad (1)$$

Swelling performance is an important study for evaluating the adsorption behavior of dressings. A gravimetric approach was carried out to determine the swelling capacity of the prepared nanomaterial. To determine the initial weight (m_i), the samples were first dried and then immersed in distilled water for 48 h. Weight was recorded for each varying imprinting period. The swelling rate was determined by applying the eqn (2):

$$\%-\mathrm{SR} = \frac{(m_f - m_i)}{m_i} \times 100 \quad (2)$$

2.6. Water vapor permeability

A standardized test for elaborating water vapor transmission (ASTM E 96-00) was followed in the water vapor permeability (WVP) analysis of electrospun meshes.[47] Briefly, the nanomaterial had a vapor permeation surface area of 3.60 cm^2 and was fixed to the aperture of the vial, which had been preloaded with 5 mL of phosphate-buffered saline (PBS). A total of five vials were used for this experiment, and they were all weighed and maintained at 32 °C. After 24 hours, weight changes were used to determine the WVP using the following equation:

$$\mathrm{WVP} = \frac{\Delta W}{tA} \quad (3)$$

Here, ΔW represents the change in water weight (g), t is the time (h), and A is the test area (the area of the vials' aperture), measured in m^2.

2.7. Mechanical properties

A tensile machine (Lhomargy 2/M) was used to assess the mechanical properties of the manufactured nanofiber material following a standard test (NFG 07-119). Experiments were performed at a test speed of 1 mm s^{-1} and a gauge length of 10 mm. The mechanical evaluation was conducted by measuring the elongation at break, the tensile strength at break, and Young's modulus. With every sample, ten distinct assays were performed.

2.8. Biological evaluation

For the different analyses, the ISO 10993-5 standard test was applied for its suitability for various biological evaluations. The nanofiber scaffolds were first cut into discs of 9 mm diameter and then sterilized for 15 minutes on a UV light source. Nickel was used as a positive control and Thermanox® material as a negative. The analyzed cells were incubated in a 5% CO_2 atmosphere, with 100% relative humidity and a temperature control of 37 °C. The various biological assessments of cell adhesion kinetics and viability were investigated in HepG2 epithelial cells.

2.8.1. Viability assay. The MTT tetrazolium test was performed to assess cell viability experiments. Cultured human HepG2 cells were poured into 96-well culture plates.

Subsequently, different samples of nanomaterials (previously cut in the form of discs) were immersed in the culture medium to initiate contact with the cells. Three periods of cell inoculation were performed (24, 48, and 72 hours). We started with cell counting after removing the culture media. Subsequently, 0.5 mg mL^{-1} of MTT medium was produced and poured into each of the culture wells, followed by an incubation period of 3 hours. After pipetting the solutions into 96-well plates, 100 mL of DMSO was transferred to each well. The different absorbances at 545 nm were then measured using an ELISA microplate reader. The average amount of relative formazan formation, accounting for the control culture, was used to express the assessed cell viability. For every test, a minimum of five distinct essays were completed in duplicate.

2.8.2. Cell kinetic adhesion assay. Adhesion is essential for tissue management and maintenance, playing a crucial role in cellular communication and regulation. Cell adhesion is the capacity of a single cell to stick to another cell or an extracellular matrix, in this case, a nanofiber scaffold mat. When designing and developing biomaterials, cellular affinity for the substrate is crucial. Improving cell adhesion may be a key moment in various diseases.[73,74] Cell adhesion assay was conducted using forty thousand developing cells which are then carefully seeded into well plates. Following that, nanofibrous sample disks were inserted into the prepared well plates. The media was taken out of each well 30, 60, and 120 minutes later, and 300 mL of *p*-NPP (*para*-nitrophenyl phosphate) solution was added. After an incubation period of 3 h, 150 mL of 1 N NaOH solution was added to halt the reaction. After that, the absorbance was measured using an Apollo LB911TM (Berold) at 405 nm. Ten independent replication tests have been performed for each established measurement.

2.8.3. Antibacterial assessment. The antibacterial performance of the different nanofiber scaffold mats was assessed using the agar disc diffusion technique.[75] Two Gram-positive bacteria (*Micrococcus luteus* NCIMB-8166 and *Staphylococcus aureus* ATCC-25923) and two Gram-negative pathogenic strains (*Escherichia coli* ATCC 35218 and *Pseudomonas aeruginosa* ATCC-33787). The strains were grown in Mueller–Hinton (MH) broth (Oxoid) at 37 °C for 24 h. Afterward, 1000 μl of each precultured suspension was spread onto plates containing MH agar nutrients, and the plates were incubated for 30 minutes at 37 °C. The nanofiber samples in the form of discs, were sterilized then deposited on the MH agar plates and left to sit at 4 °C for two hours. Following a 24-hours incubation period at 4 °C, the examined disc samples were allowed to diffuse into the MH agar. The diameter of the inhibition area that developed around the nanofiber samples was measured after examining the plates. Antimicrobial activity against bacterial strains is represented by this zone of inhibition (a clear halo around the samples). Each sample was tested in triplicate.

2.9. Statistical analysis

Differences between treatments in different conditions were investigated with analysis of variances (ANOVA) and Tukey honestly significant difference (HSD) test. All statistical analyses were tested at 0.05 level of probability, using the software Statistica (version 10). Analyzes were carried out in triplicate, and values were reported as mean ± standard deviations.

3 Results and discussion

3.1. Synthesis of the crosslinked polymer

Before the electrospinning procedure, we have prepared the crosslinked polymer. A solution of microcrystalline cellulose (MC, 3% w/v) was prepared using a mixed solvent of *N*,*N*-dimethylacetamide, and acetone (DMAC/Ac 1 : 3). The solution was heated at 70 °C and vigorously stirred until complete dissolution. 3 g of chitosan biopolymer was dissolved in a 10% acetic acid with stirring at 70 °C. Afterward, chitosan solution was added to the MC solution in a mixture of 70/30 and 90/10 with the addition of 3 g of CTR as a crosslinking agent. 1 g of sodium hypophosphite was added as a catalyst for the polyesterification reaction. The total mixture was then stirred overnight under reflux. The solution was then concentrated and the obtained product was dried in an oven.

3.2. Electrospinning procedure

The use of electrospinning as a micro- and nanofiber processing technique has increased significantly over the past 20 years. It remains the most effective way to create them in various forms applied to tissue engineering and regenerative medicine, offering cutting-edge and practical answers to the problems encountered daily.[76–78]

Previous research studies have demonstrated that according to the material and solvent selection, system setup and operating conditions vary significantly amongst material systems. The formability and shape of electrospun nanomaterials can be significantly influenced by the physical and chemical properties of the polymer solution, including viscosity, electric conductivity, and initial polymer concentration. The novelty in our study is the use of two crosslinked biopolymers which is a new challenge that is used for the first time. Therefore, this new investigation aims to exploit the additional properties provided by crosslinking to chemically, physically, and mechanically improve the properties of the produced nanomaterial. Indeed, the chemical association of the two polymers will increase the molecular weight which will influence the final nanofiber morphology. In fact, rheological characteristics like viscosity and surface tension as well as electrical characteristics like conductivity and dielectric strength are greatly influenced by molecular weight.[79] Additionally, high molecular weight polymers are beneficial to produce nanofibers because they give the appropriate viscosity. Furthermore, Casper *et al.*[80] discovered that as the polymer molecular weight increases, the fiber morphology changes, including reduced beads and irregular shape, while the pore size increases. Additionally, the fibers have a higher average diameter due to their high molecular weight. Therefore, it became possible to concept a mesh with more consistent biophysical properties.[81] Another advantage was exploited in our study which is the use of DMSO as a solvent. In addition to its great solvent potential, this solvent

has a high surface tension of about 43.7 mN m^{-1}, which is always suitable for effective electrospinning.[82] In the spinnable solution, the polymer concentration must be appropriate and well-selected. A high concentration generates extremely viscous gel and a three-dimensional network structure that prevents the solution from spinning. The low concentration produces non-stable solid nanofibers and a defective nanomaterial. An important aspect influencing the morphology of electrospun nanofibers and solution spinnability is the solution viscosity. In our study, the crosslinking process of the two biopolymers and the incorporation of the propolis biomolecule multiplies the intramolecular interactions in the crosslinked polymer which reduces the viscosity and thereby thus allows the solution to be spinnable at higher concentrations. It has been reported that homogeneous, bead-free fibers emerge when the conductivity of a solution increases. Indeed, the crosslinking of the two biopolymers could increase the conductivity of the spinnable solution. In addition, to further increase conductivity, we have added TEA known for its ability to improve this influenceable parameter. All these advantages have been exploited in order to improve the effect of the different spinnable parameters.

For the electrospinning procedure, the crosslinked polymer was dissolved (12% w/v) in DMSO with continuous stirring for 24 h. Next, propolis solution (2% w/v) was added to each polymer solution with continuous stirring for 24 h. Then the obtained solution was filtered through a PTFE Syringe Filter (Diameter 45 μm). Using a vertically set up syringe with a capacity of 10 mL, the electrospinning procedure was performed in a Yflow® Nanotech electrospinning device. The electrospinning process was carried out at a voltage of 20/−20 kV (high voltage injector/high voltage collector) and the distance from the stationary collector plate was kept 15 cm from the blunt needle tip of the syringe. The flow rate was fixed to 0.4 μl min^{-1}. The needle diameter selected was 0.4 mm. Continuous nanofibers that successfully formed were collected across the aluminum foil covering the stationary horizontal collector plate.

The resulting polymer nanofibers with an average diameter of less than 500 nm were collected at lengths up to 50.5 cm. The orientation of the gathered nanofibers was mostly perpendicular to the plate, or nearly so. The resulting nanomaterial exhibits good resistance so it could subsequently undergo consolidation to better improve its mechanical characteristics, an important attribute for effective application as a wound dressing scaffold. This may be due to the use of two polysaccharide polymers chemically crosslinked and with relatively high concentrations in addition to the selection of the different parameters.

3.3. Viscosity measurement

Viscosity is the most important solution parameter having a direct influence on the morphology of electrospun nanofibers. The viscosity of the solution is closely related to the concentration of the solution and the molecular weight of the polymer.[83] The MC/CS mixing ratio may be the only factor influencing the viscosity of the solution because the concentration of the MC/CS solution is maintained at 12%. Table 1 displays the measured shear viscosity for the two mixing ratios at a constant shear rate of 100 s^{-1}. The viscosities for the blends 90/10 and 70/30 were 174.4 and 192.2 mPa s, respectively. The viscosity was improved significatively with increasing chitosan content ($p < 0.05$). This increase in viscosity could influence the electrospinability and morphology of the fibers.[84]

3.4. Contact angle measurement

An effective wound dressing must be hydrophilic to absorb exudates and avoid rapid bacterial colonization which favors hydrophobic surfaces. Hydrophilicity also plays a major role in cell adhesion, proliferation, and migration.[85] For the contact angle evaluation of the two blend ratios of MC/CS 90/10 and 70/30, two solvent tests water and glycerol were used. Results in Fig. 1 show relatively low contact angles (<90°) for the different samples with the two solvents test used, this demonstrated the hydrophilic character of the produced nanomaterials. The blend ratio of 70/30 revealed a lower contact angle than the ratio of 90/10, so with the addition of more chitosan the contact angle decreased from 62.12 to 58.22° with water and from 78.24 to 70.14° with glycerol solvent test that has a lower tension surface than water. The improvement in hydrophilicity was expected to be linked to the hydrophilic properties of chitosan and the crosslinker used.[86]

3.5. Swelling and water uptake capacity

To accelerate wound healing, the dressing's ability to maintain a suitable moist environment in the wound areas is indicated by its water absorption and retention.[87] Furthermore, a dry environment promotes cell death, which results in crust and scar development. Because new tissue fibroblasts must break through this crust, healing takes longer and requires more energy.[88,89] The wound environment could be maintained *via* gas exchange through the pores of the material and *via* absorption of exudates, which promotes bacterial proliferation and delays the wound healing process.[90] The results in Table 1 show higher swelling behavior for the two prepared nanomaterials, which are 436.12 and 438.44% for the 90/10 and 70/30 mixing ratios, respectively. Unlike the study of the contact angle where the difference was more significant particularly with glycerol ($p = 0.01 < 0.05$) since the influence of the hydrophilic nature of the polymers played a decisive role. Here, for swelling, the result depends on the hydrophilicity of the polymers, but porosity could also affect the degree of swelling. Thus, for the material with the 70/30 blend ratio, the addition of more chitosan increases the degree of crosslinking and thus allows a denser structure and decreases the pore sizes, and therefore the water molecules have more difficulty in entering. This competition between a more hydrophilic character and a more compact structure with the addition of more chitosan is behind these close values in swelling capacity.

3.6. Water vapor permeability

A perfect wound dressing has to ensure a sufficient rate of water vapor permeability (WVP) to effectively protect the wound from

Table 1 Physicochemical characteristics of the produced nanomaterials[a]

Nanomaterial's blend ratios	Viscosity (mPa s)	Average fiber diameter (nm)	Contact angle (°) water/glycerol	Swelling degree (%)	WVP (g per m^2 per day)
MC/CS: 90/10	174.4*	431.4	62.12/78.24*	436.12	1735.12*
MC/CS: 70/30	192.2*	441.2	58.22/70.14*	438.44	1698.52*

[a] Data presented as mean ± SD. Mean values followed by (*) means that results are significantly different at $p < 0.05$.

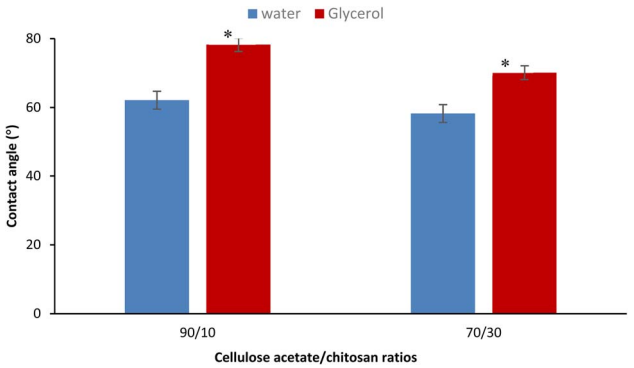

Fig. 1 Contact angle assessment of the different nanofiber scaffolds using water and glycerol as solvent tests. Data presented as mean ± SD. Mean values followed by (*) means that results are significantly different at $p < 0.05$.

an overly dry or moist environment.[91] The results in Table 1 showed relatively high WVP rates for both samples produced. Indeed, the nanomaterial with a blend ratio of 90/10 had a permeability of 1735.12 g per m^2 per day while the sample with a blend ratio of 70/30 revealed a slightly lower permeability of 1698.52 gm^{-2}day. This significative decrease ($p < 0.05$) with the addition of more chitosan could be caused by the smaller fiber diameter and high mesh porosity. The WVP values of the two prepared nanomaterials are highly relevant because, to ensure an appropriate moisture level and avoid wound dehydration, an ideal wound should have a WVP between 1500 and 2500 g per m^2 per day, and burned or injured skin should have a WVP of between 279 and 5138 g per m^2 per day.[92,93] The calculated WVPs are very close to the recommended values and higher than those of the majority of commercial dressings, including Tegaderm® (491 g per m^2 per day), Dermiflex® (76 g per m^2 per day) and OpSite® (792 g per m^2 per day).[94]

3.7. Nanofiber diameter and morphology

Among the essential functions of an ideal dressing for skin regeneration, covering and protecting the wound from bacterial infections and maintaining a favorable humid environment. This could be achievable by the use of electrospun fibers due to their porosity. This porosity must be high (60–90%) with great interconnectivity facilitating the required passage of nutrients, oxygen, and cells.[95] SEM analysis was performed on two different blend ratios of MC and chitosan polymers (90/10 and 70/30). Fig. 2 shows the different micrographs at various magnifications. Both prepared scaffolds display homogeneous and bead-free nanofibrous structures. The nanofibers are continuous with a random orientation. Additionally, the nanofiber mats exhibit slight shrinkage from their initial sizes which was therefore linked to a decrease in inter-fibrous pore size.[96]

Fig. 3 shows the fiber diameter distribution at the two prepared blend ratios. The calculated average nanofiber diameters for the MC/CTR/CS blend ratios at 90/10 and 70/30 were 431.4 and 441.2 nm, respectively. The results revealed that larger nanofibers with narrow diameter distribution appeared as the amount of chitosan increased, and these findings were consistent with those reported in the literature on natural polymer blends.[97] As demonstrated by our previously mentioned viscosity data, large fiber diameters may be related to an increase in the viscosity of the electrospun solution upon the addition of chitosan, thereby inducing increased jet resistance for the production of thicker fibers. Furthermore, when the concentration of chitosan increased, a more uniform distribution of the nanofibers suggested an improvement in the electrospinability of the MC/CS solution.

3.8. FTIR analysis

Different functional groups were identified by FT-IR analysis *via* the ATR mode, to study the composition of the produced electrospun nanomaterial and in particular to evaluate the chemical grafting between the microcrystalline cellulose and the chitosan biopolymer. We examined the spectra of the biopolymers before and after the crosslinking procedure.

Fig. 4 shows the spectra of the raw materials and the produced electrospun nano-fibers. For the different spectra, we notice the presence of some characteristic bands of chemical groups that belong to both the raw and prepared materials. These absorption bands include a broad band at 3271.67 cm^{-1} attributed to the O–H stretching absorption band and intramolecular hydrogen bonds and a band at approximately 2907.87 cm^{-1} as-signed to C–H symmetric and asymmetric stretch vibrations. The C–O–C stretching vibration of the glycosidic fraction of the different materials was detected in an intense band around 1035 cm^{-1}.[98,99] Absorption bands corresponding to the C–O–C glycosidic bonds of pyranose are identified within the region of 1000–1100 cm^{-1}. The band appearing at 1645 cm^{-1} corresponds to the C=O stretching of amide I, while at 1325 cm^{-1} we notice the presence of the band of the C–N stretching of amide III. These stretching patterns are indicative of the remaining *N*-acetyl groups from chitosan. Additionally, the primary amine's N–H bending is correlated with the peak at 1589 cm^{-1}.[100] A new main band appears only on the spectrum of the produced nanomaterial at 1714 cm^{-1} which

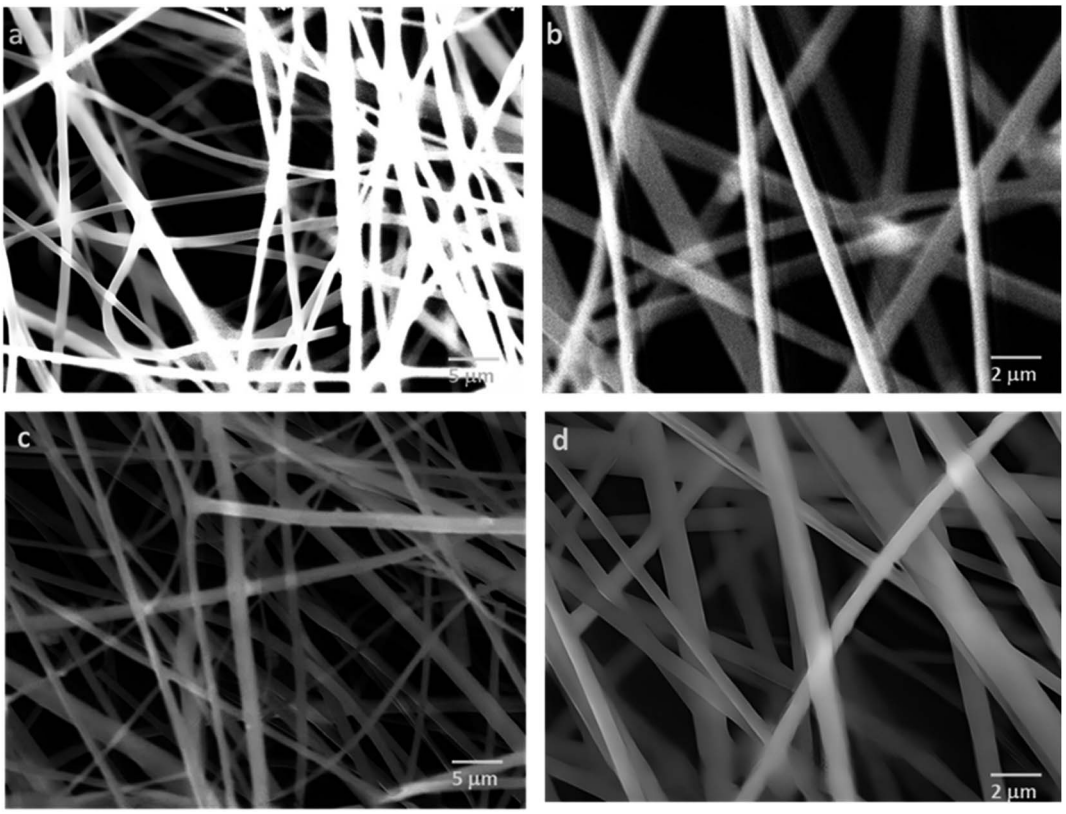

Fig. 2 SEM micrographs of MC/CTR/CS crosslinked nanofiber mats: (a) blend ratio 90/10, magnification 5000×, (b) blend ratio 70/30, 10 000×, (c) blend ratio 70/30, 5000×, (d) blend ratio 70/30, 10 000×.

is assigned to both the ester and amide groups resulting from the crosslinking reaction between the microcrystalline cellulose and the chitosan polymers.[101,102] This band confirmed the success of polyesterification and amidification reactions before nanofiber conception and the stability of the crosslinked polymers after the electrospinning procedure.

3.9. Mechanical evaluation

An effective dressing must have appropriate mechanical properties to withstand physiological stresses and maintain its properties throughout its use.[103] Since a moist environment is typical of wounds, the tensile properties were performed in a wet state.

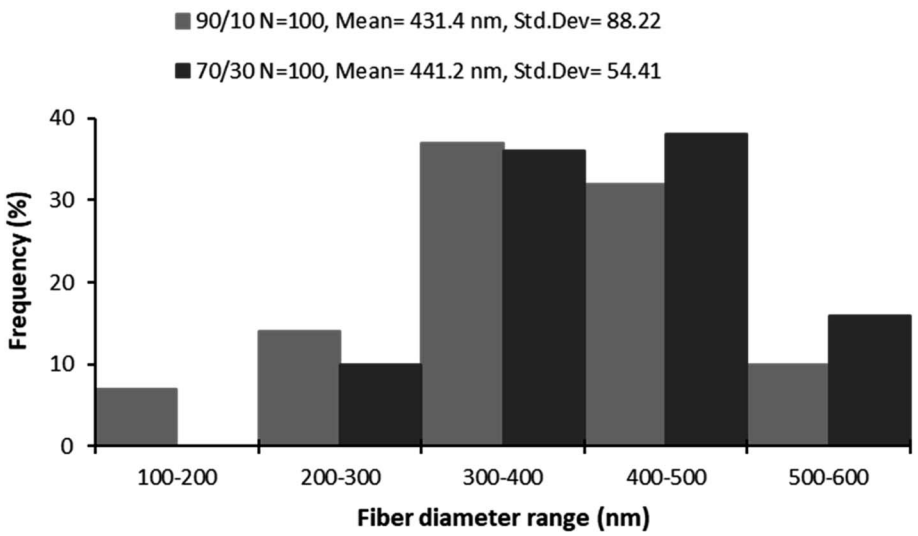

Fig. 3 Diagram of nanofiber diameter distributions of prepared nanomaterials at different blend ratios.

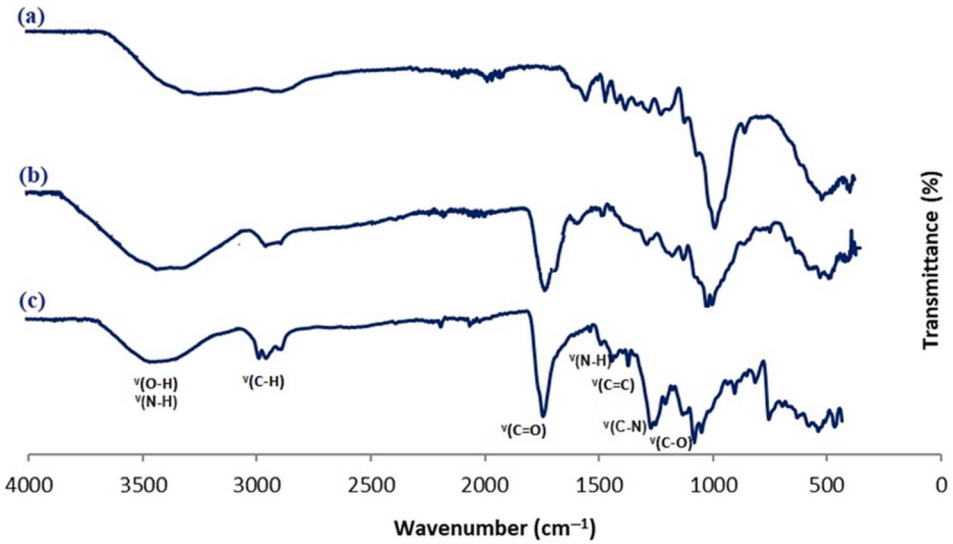

Fig. 4 FT-IR spectra of MC polymer (a), crosslinked MC/CS polymer (b), and nanofiber scaffold material with blend ratio 70/30 (c).

The different mechanical characteristics such as tensile strength, Young's modulus, and elongation at break are shown in Table 2. The results revealed high values of tensile strength and Young's modulus for the two nanomaterials produced. Increasing the amount of chitosan in the sample provides higher tensile strength and Young's modulus, this can be explained by the increased crosslinking rate allowing for a denser structure.[104] The incorporation of 30% chitosan *versus* 10% results in an increase in tensile strength of 11% and 14% in Young's modulus. Therefore, increasing the chitosan level and therefore the degree of crosslinking led to stiffer and more robust nanofiber structures. Furthermore, the elongation at break value was slightly higher for nanomaterials containing 10% chitosan, which meant that increasing the amount of chitosan tends to make the material more brittle and less flexible. Therefore, we could adjust the different mechanical properties simply by modifying the blend ratio rate of the electrospun polymers.

3.10. Biological assessments

Good biocompatibility efficiency is an essential and desired characteristic for dressing biomaterials in various biomedical applications. They must support efficient cellular metabolic activity and justify the absence of cytotoxicity towards human cells.

3.10.1. Viability assays. Human HepG2 epithelial cells were used to perform cell viability assays on the different nanofiber scaffold mats evaluated. Effective cell proliferation in the samples examined is indicated by the presence of MTT (yellow tetrazolium salt) metabolic activity in contact with the cells, which generates an absorbance characteristic of blue formazan. The variation in absorbance observed is directly linked to the vitality of the cells, allowing the sample to be optimally adapted to biological metabolism. Maximum cell viability was determined by setting the absorbance, measured using the control, to 100%. The results of the cell viability tests for the samples with different blend ratios are shown in Fig. 5. We notice a clear improvement in the cell metabolic activity with the two nanofiber scaffolds compared to the control ($p < 0.05$). This can be explained by the presence of the chitosan and the propolis bioactive molecules known for their excellent biocompatibility potential.[105,106] Furthermore, the nanofiber structure with a porosity allowing the penetration of oxygen and nutrients is behind these outcomes. However, to further improve cell viability performance we must preserve a good porosity and

Table 2 Mechanical characteristics of the produced nanomaterials

Nanomaterial's blend ratios	Tensile strength (MPa)	Young's modulus (MPa)	Elongation at break (%)
MC/CS: 90/10	7.42	174.61	11.52
MC/CS: 70/30	8.27	199.08	10.31

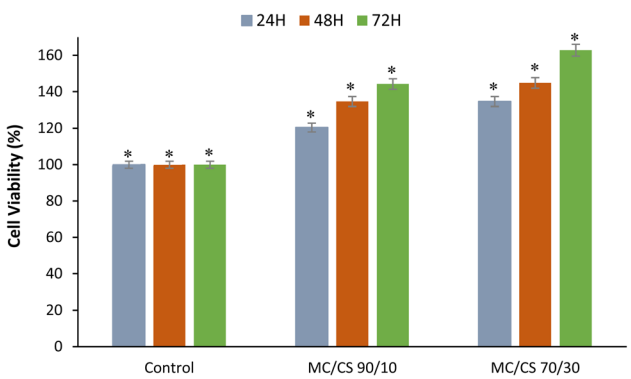

Fig. 5 Cell viability assay on the different nanofiber scaffolds using HepG2 epithelial fibroblast cells. Data presented as mean ± SD. Mean values followed by (*) means that results are significantly different at $p < 0.05$.

produce nanofibers that mimic the natural extracellular matrix (ECM) with a diameter of 10–300 nm.[107] Results revealed a clear increase in fibroblast metabolic activity for the sample with a blend of 70/30 compared to the sample with a blend of 90/10 with all the varied periods ($p < 0.05$). This significant variation can be associated with their higher fiber diameter when compared to the other condition, which resulted in a less dense structure, that facilitate the deep penetration of the cells. Analogous cases are reported in other investigations.[108] This improvement with the samples having more amounts of chitosan may potentially be explained by the ability of the chitosan to boost cell proliferation and promote chondrocyte retention, which increases cell metabolic activity.[109] In addition, results revealed the gradual increase of the cell viability behavior with the period of contact with fibroblast cells, which can be related to the prolonged release of the propolis incorporated in the polymeric nanofiber network.

3.10.2. Cell adhesion assays. Results in Fig. 6 revealed a clear improvement of the cell adhesion with the nano-fiber scaffolds in comparison to the control. The presence of the chitosan and the propolis increased the cell adhesion to the fibroblasts. The nanostructured design of the nanofiber mats could also enhance the cell adhesion ability. This confirmed the absence of any cytotoxicity and the good biocompatibility of the produced nanofiber mats. Results showed the improvement in fibroblast integration and spread with the designed nanofibers confirmed by the increase in the cell adhesion rates. Over the different adhesion times the adhesion passes from a surface adhesion (30 min) to integration in the nanofiber structure (60 min) and proliferation over the electrospun structure after 120 min of cell contact. Results show an increase in the adhesion rates over contact time with fibroblasts. The samples containing further chitosan amount demonstrated an improved adhesion behavior, the differences are more significative after 60 and 120 min of cell contact ($p < 0.05$). Another aspect can be assigned to the higher hydrophilic character of the made nanofiber scaffolds previously confirmed in the wettability study. Thanks to the different hydrophilic groups contained in the two biopolymers and the propolis and the capability of the nucleophilic functions (NH_2) to establish chemical bonds to cells, cell attachment, and proliferation were significantly improved.[110,111] In addition, the combination of the two biological polymers and the bioactive propolis molecule may offer an adequate environment in electrospun nanofibers, favorable for cell migration and infiltration, thus fostering skin regeneration.

3.10.3. Antibacterial activity. Antimicrobial tests were carried out using 2 Gram-positive bacterial strains; *Micro-coccus luteus* (Ml) and *Staphylococcus aureus* (Sa), and 2 Gram-negative bacteria; *Escherichia coli* (Ec) and *Pseudomonas aeruginosa* (Pa). The antimicrobial activity was performed on the cellulosic nanomaterial as a control and on the nanomaterials of cellulose and chitosan without propolis and on the two different electrospun nanofibers of cellulose/chitosan/propolis produced with the MC/CS blend ratios of 90/10 and 70/30. The activity was assessed by the inhibitory diameter zone that developed around the samples. Results in Fig. 7 revealed no activity for the cellulosic nanofibers tested as a control. On the other hand, the nanofibers made of cellulose and chitosan exhibited a moderate activity against the different bacteria. With the presence of propolis in the electrospun samples we noticed the presence of significant antimicrobial activity for the two different prepared samples and against all the selected bacterial strains ($p < 0.05$). Therefore, the recorded antibacterial activity is caused by the potential of the biopolymer chitosan and is further intensified in the presence of propolis. We noticed that by increasing the amount of chitosan biopolymer in the nanofiber structure, the antibacterial behavior became more pronounced especially with the Gram-positive strains ($p < 0.05$). This could be explained by the antibacterial properties of chitosan and the propolis biomolecule which is more prevalent and incorporated in the nanofiber sample containing more chitosan biopolymer. The

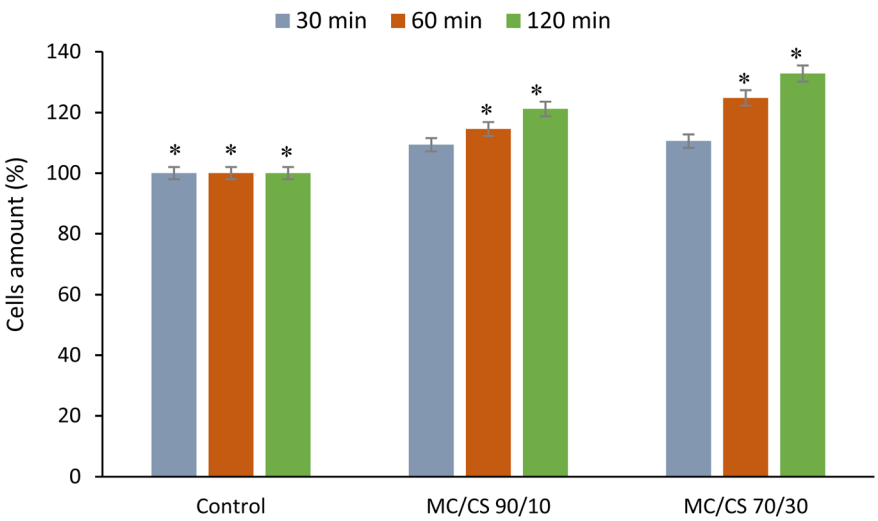

Fig. 6 Cell adhesion assay on the different nanofiber scaffolds using HepG2 epithelial fibroblast cells. Data presented as mean ± SD. Mean values followed by (*) means that results are significantly different at $p < 0.05$.

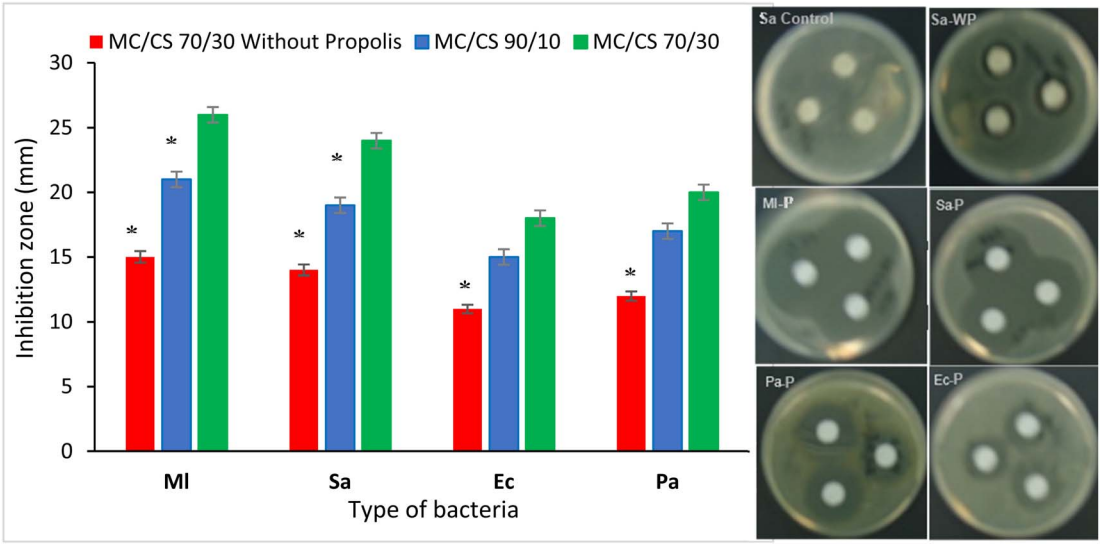

Fig. 7 Antibacterial assays of the different nanofiber scaffolds at the various blend ratios of MC/CS biopolymers against different bacterial strains *via* the evaluation of the inhibition zone surrounding the samples. Data presented as mean ± SD. Mean values followed by (*) means that results are significantly different at $p < 0.05$ (in antibacterial screening images control: cellulose nanomaterial, -P: sample with propolis and -WP: sample without propolis).

results are in line with literature where propolis which through different mechanisms mainly structural ones, causes cell lysis and bacterial cell membrane damage leading to cell death and its action is more effective against Gram-positive bacteria.[112,113] Chitosan biopolymer had demonstrated considerable antibacterial activity. The first and most generally recognized model involves that chitosan interacts electrostatically with the anionic surface of both Gram-positive and Gram-negative bacteria, allowing the destruction of the cell wall membrane.[114,115]

4 Conclusion

The primary goal of this research study was to develop a multifunctional dressing by exploring, for the first time, the electrospinning process using two natural biopolymers, cellulose acetate, and chitosan, previously crosslinked and incorporated with propolis as an active biological molecule. The nanofiber mats were created, characterized, and analyzed in terms of effectiveness as drug delivery systems and functional wound dressings. MC/CS nanofiber mats incorporated with propolis biomolecule at various polymer blend ratios were efficiently created by an electrospinning procedure. Different machine parameters were optimized to obtain nanofiber scaffolds with excellent strength and structures. SEM evaluation of the different prepared nanomaterials revealed homogeneous and bead-free nanofibrous structures, with well-defined morphology and a random deposition that could accurately mimic the extracellular matrix of native skin. The calculated average nanofiber diameters for the MC/CS blend ratios at 90/10 and 70/30 were 431.4 and 441.2 nm, respectively. The results showed that larger nanofibers with narrow diameter distribution emerged as the chitosan amount increased. Furthermore, the different electrospun nanofiber conditions provide an appropriate porosity, and improved hydrophilic and swelling proprieties to act as an efficient wound dressing. The prepared nanomaterials had a significant and close water vapor permeability of about 1735.12 and 1698.52 g per m^2 per day for the two blend ratios of 90/10 and 70/30, respectively. These high WVP values are very close to the recommended values and above all higher than those of most commercial dressings, and they are therefore ideal for the dressings to effectively protect the wound from an overly dry or moist environment. FT-IR analysis confirmed the success of the chemical crosslinking *via* both polyesterification and amidification reactions between the two polymers before nanofiber conception and the stability of the crosslinked polymers after the electrospinning process. The designed nanomaterials possessed excellent mechanical properties depending on the chitosan content. The two nanomaterials developed showed high values of tensile strength and Young's modulus. The incorporation of 30% chitosan *versus* 10% results in an increase in tensile strength of 11% and 14% in Young's modulus. Therefore, we could adjust the different mechanical properties simply by modifying the blend ratio rate of the electrospun polymers. Biological evaluations using HepG2 epithelial fibroblast cells *via* viability and kinetic adhesion assays showed the non-toxicity and excellent biocompatibility of the designed dressings. Moreover, at different cell contact times, the nanofiber scaffold samples with various mixing ratios of MC and chitosan biopolymers demonstrated effective cell adhesion performance. Antimicrobial assays *via* agar diffusion experiments using different Gram-positive and Gram-negative bacterial strains revealed a significant bactericidal performance that increased with the rise of chitosan and propolis amounts in the nanofiber composite scaffold. Thanks to the multiple biological and therapeutic properties of the

chitosan and the propolis and the promising characteristic of the electrospun nanomaterial to mimic ECM, the successful production of electrospinning crosslinked biopolymers incorporated with bioactive molecules will offer a promising alternative, to treat chronic and acute wounds. Furthermore, by controlling the degree of polymer mixing, nanofibers can achieve a certain balance between their mechanical characteristics and their biofunctionality. As a perspective, additional biological, bacteriological, and anticancer evaluations of the designed nanofiber dressings could be investigated.

Data availability

The authors confirm that the data supporting the findings of this study are available within the article.

Author contributions

Data curation, Y. E.-G. and G. A. A. and A. S. A.; formal analysis, Y. E.-G. and G. A. A.; A. S. A.; investigation, Y. E.-G. and A. S. A.; methodology, Y. E.-G.; project administration, Y. E.-G.; software, Y. E.-G. and G. A. A.; supervision, Y. E.-G.; validation, Y. E.-G.; A. S. A.; writing – original draft, Y. E.-G. and G. A. A. and A. S. A.; writing – review & editing, Y. E.-G. All authors have read and agreed to the published version of the manuscript.

Conflicts of interest

The authors declare no conflict of interest.

Acknowledgements

The authors gratefully acknowledge Qassim University, represented by the Deanship of Scientific Research, on the financial support for this research under the number COS-2022-1-1-J-27033 during the academic year 1444 AH/2022 AD.

References

1 H. He, D.-L. Xia, Y.-P. Chen, X.-D. Li, C. Chen, Y.-F. Wang, L. Shen, Y.-L. Hu and H.-Y. Gu, Evaluation of a two-stage antibacterial hydrogel dressing for healing in an infected diabetic wound, *J. Biomed. Mater. Res., Part B*, 2017, **105**(7), 1808–1817.

2 S. Nemati, Sj. Kim, Y. M. Shin and H. Shin, Current progress in application of polymeric nanofibers to tissue engineering, *Nano Convergence*, 2019, **6**, 36.

3 A. B. Karakullukcu, E. Taban and O. O. Ojo, Biocompatibility of biomaterials and test methods: a review, *Mater. Test.*, 2023, **65**(4), 545–559.

4 W. Al-Zyoud, D. Haddadin, S. A. Hasan, H. Jaradat and O. Kanoun, Biocompatibility Testing for Implants: A Novel Tool for Selection and Characterization, *Materials*, 2023, **16**, 6881.

5 P. Singh, K. R. Singh, A. K. Yadav, J. Singh, P. R. Solanki and R. P. Singh, Carbon-based nanostructured materials for effective strategy in wound management, in *Nanotechnological Aspects for Next-Generation Wound Management*, Academic Press, 2024, pp. 193–218.

6 F. Abaszadeh, M. H. Ashoub, G. Khajouie and M. Amiri, Nanotechnology development in surgical applications: recent trends and developments, *Eur. J. Med.Res.*, 2023, **28**, 537.

7 G. Zafaripour, M. Yazdchi, A. A. Alizadeh, M. G. Nejad, D. A. Dehkordi and D. T. Semirumi, Fabrication and evaluation of 3D bio-scaffold wound dressings for monitoring of chronic pH wounds using fuzzy logic analysis, *Mater. Sci. Eng. B*, 2023, **294**, 116542.

8 A. G. Abdelaziz, H. Nageh, S. M. Abdo, M. S. Abdalla, A. A. Amer, A. Abdal-hay and A. Barhoum, A Review of 3D Polymeric Scaffolds for Bone Tissue Engineering: Principles, Fabrication Techniques, Immunomodulatory Roles, and Challenges, *Bioengineering*, 2023, **10**, 204.

9 M. Entezari, G. G. Y. Abad, B. Sedghi, R. Ettehadi, S. Asadi, R. Beiranvand, N. Haratian, S. S. Karimian, A. Jebali, R. Khorrami and M. A. Zandieh, Gold nanostructure-mediated delivery of anti-cancer agents: Biomedical applications, reversing drug resistance, and stimuli-responsive nanocarriers, *Environ. Res.*, 2023, **225**, 115673.

10 Y. Zhang, K. Poon, G. S. P. Masonsong, Y. Ramaswamy and G. Singh, Sustainable Nanomaterials for Biomedical Applications, *Pharmaceutics*, 2023, **15**, 922.

11 A. Soni, M. P. Bhandari, G. K. Tripathi, P. Bundela, P. K. Khiriya, P. S. Khare, M. K. Kashyap, A. Dey, B. Vellingiri, S. Sundaramurthy and A. Suresh, Nano-biotechnology in tumor and cancerous disease: A perspective review, *J. Cell. Mol. Med.*, 2023, **27**(6), 737–762.

12 K. Kuperkar, L. I. Atanase, A. Bahadur, I. C. Crivei and P. Bahadur, Degradable Polymeric Bio(nano)materials and Their Biomedical Applications: A Comprehensive Overview and Recent Updates, *Polymers*, 2024, **16**, 206.

13 D. Di Francesco, A. Pigliafreddo, S. Casarella, L. Di Nunno, D. Mantovani and F. Boccafoschi, Biological Materials for Tissue-Engineered Vascular Grafts: Overview of Recent Advancements, *Biomolecules*, 2023, **13**, 1389.

14 J. Chen, D. Zhang, L.-P. Wu and M. Zhao, Current Strategies for Engineered Vascular Grafts and Vascularized Tissue Engineering, *Polymers*, 2023, **15**, 2015.

15 Z. Jiang, Z. Zheng, S. Yu, Y. Gao, J. Ma, L. Huang and L. Yang, Nanofiber Scaffolds as Drug Delivery Systems Promoting Wound Healing, *Pharmaceutics*, 2023, **15**, 1829.

16 R. Hama, J. W. Reinhardt, A. Ulziibayar, T. Watanabe, J. Kelly and T. Shinoka, Recent Tissue Engineering Approaches to Mimicking the Extracellular Matrix Structure for Skin Regeneration, *Biomimetics*, 2023, **8**, 130.

17 T. He, Y. Xiao, Z. Guo, Y. Shi, Q. Tan, Y. Huang and H. Xie, Modulation of Macrophage Function by Bioactive Wound Dressings with an Emphasis on Extracellular Matrix-Based Scaffolds and Nanofibrous Composites, *Pharmaceutics*, 2023, **15**, 794.

18 S. Farzamfar, E. Elia, M. Richer, S. Chabaud, M. Naji and S. Bolduc, Extracellular Matrix-Based and Electrospun Scaffolding Systems for Vaginal Reconstruction, *Bioengineering*, 2023, **10**, 790.

19 M. Z. A. Zulkifli, D. Nordin, N. Shaari and S. K. Kamarudin, Overview of Electrospinning for Tissue Engineering Applications, *Polymers*, 2023, **15**, 2418.
20 G. G. Flores-Rojas, B. Gómez-Lazaro, F. López-Saucedo, R. Vera-Graziano, E. Bucio and E. Mendizábal, Electrospun Scaffolds for Tissue Engineering: A Review, *Macromol*, 2023, **3**, 524–553.
21 P. Wang, H. Lv, X. Cao, Y. Liu and D.-G. Yu, Recent Progress of the Preparation and Application of Electrospun Porous Nanofibers, *Polymers*, 2023, **15**, 921.
22 X. Wen, J. Xiong, S. Lei, L. Wang and X. Qin, Diameter Refinement of Electrospun Nanofibers: From Mechanism, Strategies to Applications, *Adv. Fiber Mater.*, 2022, **4**, 145–161.
23 J. Song, X. Lin, L. Y. Ee, S. F. Y. Li and M. Huang, A Review on Electrospinning as Versatile Supports for Diverse Nanofibers and Their Applications in Environmental Sensing, *Adv. Fiber Mater.*, 2023, **5**, 429–460.
24 P. R. Patel and R. V. N. Gundloori, A review on electrospun nanofibers for multiple biomedical applications, *Polym. Adv. Technol.*, 2023, **34**(1), 44–63.
25 Y. EL-Ghoul, F. M. Alminderej, F. M. Alsubaie, R. Alrasheed and N. H. Almousa, Recent Advances in Functional Polymer Materials for Energy, Water, and Biomedical Applications: A Review, *Polymers*, 2021, **13**, 4327.
26 M. Kitsara, O. Agbulut, D. Kontziampasis, Y. Chen and P. Menasché, Fibers for hearts: A critical review on electrospinning for cardiac tissue engineering, *Acta Biomater.*, 2017, **48**, 20–40.
27 W. Han, L. Wang, Q. Li, B. Ma, C. He, X. Guo, J. Nie and G. Ma, A review: Current status and emerging developments on natural polymer-based electrospun fibers, *Macromol. Rapid Commun.*, 2022, **43**(21), 2200456.
28 Y. Mao, W. Shen, S. Wu, X. Ge, F. Ao, Y. Ning, Y. Luo and Z. Liu, Electrospun polymers: Using devices to enhance their potential for biomedical applications, *React. Funct. Polym.*, 2023, **186**, 105568.
29 F. Zhang and M. W. King, Biodegradable polymers as the pivotal player in the design of tissue engineering scaffolds, *Adv. Healthcare Mater.*, 2020, **9**(13), 1901358.
30 M. C. Socci, G. Rodríguez, E. Oliva, S. Fushimi, K. Takabatake, H. Nagatsuka, C. J. Felice and A. P. Rodríguez, Polymeric Materials, Advances and Applications in Tissue Engineering: A Review, *Bioengineering*, 2023, **10**, 218.
31 J. Oztemur, S. Ozdemir, H. Tezcan-Unlu, G. Cecener, H. Sezgin and I. Yalcin-Enis, Investigation of biodegradability and cellular activity of PCL/PLA and PCL/PLLA electrospun webs for tissue engineering applications, *Biopolymers*, 2023, **114**(11), e23564.
32 J. Oztemur, S. Ozdemir and I. Yalcin-Enis, Effect of blending ratio on morphological, chemical, and thermal characteristics of PLA/PCL and PLLA/PCL electrospun fibrous webs, *Int. J. Polym. Mater. Polym. Biomater.*, 2023, **72**(10), 793–803.
33 J. R. Dias, A. Sousa, A. Augusto, P. J. Bártolo and P. L. Granja, Electrospun Polycaprolactone (PCL) Degradation: An In Vitro and In Vivo Study, *Polymers*, 2022, **14**, 3397.
34 V. Allizond, G. Banche, M. Salvoni, M. Malandrino, C. Cecone, A. M. Cuffini and P. Bracco, Facile One-Step Electrospinning Process to Prepare AgNPs-Loaded PLA and PLA/PEO Mats with Antibacterial Activity, *Polymers*, 2023, **15**, 1470.
35 R. Xu, Y. Fang, Z. Zhang, Y. Cao, Y. Yan, L. Gan, J. Xu and G. Zhou, Recent Advances in Biodegradable and Biocompatible Synthetic Polymers Used in Skin *Wound Healing*, *Materials*, 2023, **16**, 5459.
36 A. S. Gill, M. Sood, P. K. Deol and I. P. Kaur, Synthetic polymer-based electrospun scaffolds for wound healing applications, *J. Drug Delivery Sci. Technol.*, 2023, **89**, 105054.
37 H. Y. Vargas-Molinero, A. Serrano-Medina, K. Palomino-Vizcaino, E. A. López-Maldonado, L. J. Villarreal-Gómez, G. L. Pérez-González and J. M. Cornejo-Bravo, Hybrid Systems of Nanofibers and Polymeric Nanoparticles for Biological Application and Delivery Systems, *Micromachines*, 2023, **14**, 208.
38 L. Janů, E. Dvořáková, K. Polášková, M. Buchtelová, P. Ryšánek, Z. Chlup, T. Kruml, O. Galmiz, D. Nečas and L. Zajíčková, Enhanced Adhesion of Electrospun Polycaprolactone Nanofibers to Plasma-Modified Polypropylene Fabric, *Polymers*, 2023, **15**, 1686.
39 J. Ponphaiboon, W. Krongrawa, W. W. Aung, N. Chinatangkul, S. Limmatvapirat and C. Limmatvapirat, Advances in Natural Product Extraction Techniques, Electrospun Fiber Fabrication, and the Integration of Experimental Design: A Comprehensive Review, *Molecules*, 2023, **28**, 5163.
40 A. Al-Abduljabbar and I. Farooq, Electrospun Polymer Nanofibers: Processing, Properties, and Applications, *Polymers*, 2023, **15**, 65.
41 M. Y. Razzaq, M. Balk, M. Mazurek-Budzyńska and A. Schadewald, From Nature to Technology: Exploring Bioinspired Polymer Actuators via Electrospinning, *Polymers*, 2023, **15**, 4029.
42 N. Stoyanova, N. Nachev and M. Spasova, Innovative Bioactive Nanofibrous Materials Combining Medicinal and Aromatic Plant Extracts and Electrospinning Method, *Membranes*, 2023, **13**, 840.
43 L. Pisklákova, K. Skuhrovcová, T. Bártová, J. Seidelmannová, Š. Vondrovic and V. Velebný, Trends in the Incorporation of Antiseptics into Natural Polymer-Based Nanofibrous Mats, *Polymers*, 2024, **16**, 664.
44 A. Guzmán-Soria, V. Moreno-Serna, D. A. Canales, C. García-Herrera, P. A. Zapata and P. A. Orihuela, Effect of Electrospun PLGA/Collagen Scaffolds on Cell Adhesion, Viability, and Collagen Release: Potential Applications in Tissue Engineering, *Polymers*, 2023, **15**, 1079.
45 A. Ravindran Girija, X. Strudwick, S. Balasubramanian, V. Palaninathan, S. D. Nair and A. J. Cowin, Collagen Functionalization of Polymeric Electrospun Scaffolds to Improve Integration into Full-Thickness Wounds, *Pharmaceutics*, 2023, **15**, 880.

46 V. Chernonosova, M. Khlebnikova, V. Popova, E. Starostina, E. Kiseleva, B. Chelobanov, R. Kvon, E. Dmitrienko and P. Laktionov, Electrospun Scaffolds Enriched with Nanoparticle-Associated DNA: General Properties, DNA Release and Cell Transfection, *Polymers*, 2023, **15**, 3202.
47 D. Soukarie, L. Nocete, A. M. Bittner and I. Santiago, DNA data storage in electrospun and melt-electrowritten composite nucleic acid-polymer fibers, *Mater. Today Bio*, 2024, **24**, 100900.
48 M. Li, P. Zhang, Q. Wang, N. Yu, X. Zhang and S. Su, Electrospinning Novel Sodium Alginate/MXene Nanofiber Membranes for Effective Adsorption of Methylene Blue, *Polymers*, 2023, **15**, 2110.
49 B. Cecchini, R. Rovelli, L. Zavagna, B. Azimi, T. Macchi, E. Kaya, S. Esin, L. Bruschini, M. Milazzo, G. Batoni and S. Danti, Alginate-Based Patch for Middle Ear Delivery of Probiotics: A Preliminary Study Using Electrospray and Electrospinning, *Appl. Sci.*, 2023, **13**, 12750.
50 L. Lin, H. Fang, C. Li, J. Dai, M. Alharbi and H. Cui, Advancing gelatin/cinnamaldehyde O/W emulsions electrospinability: Role of soybean lecithin in core-shell nanofiber fabrication, *Food Chem.*, 2024, **449**, 139305.
51 Y. Cho, H. Jeong, B. Kim, J. Jang, Y.-S. Song and D. Y. Lee, Electrospun Poly(L-Lactic Acid)/Gelatin Hybrid Polymer as a Barrier to Periodontal Tissue Regeneration, *Polymers*, 2023, **15**, 3844.
52 X. Wang, Z. Bai, K. Li, J. Dong, H. Zhang, X. Liu, W. Han and Q. Li, Bioinspired PLCL/Elastin Nanofibrous Vascular Tissue Engineering Scaffold Enhances Endothelial Cells and Inhibits Smooth Muscle Cells, *Biomacromolecules*, 2023, **24**(6), 2741–2754.
53 E. Lamei and M. Hasanzadeh, Concurrent electrospinning of microporous metal-organic framework-laden casein/PVA nanofibrous composites for potential antibacterial wound dressing applications, *Int. J. Polym. Mater. Polym. Biomater.*, 2024, **73**(8), 637–645.
54 M. Liu, S. Zhang, Y. Ye, X. Liu, J. He, L. Wei, D. Zhang, J. Zhou and J. Cai, Robust Electrospinning-Constructed Cellulose Acetate@Anthocyanin Ultrafine Fibers: Synthesis, Characterization, and Controlled Release Properties, *Polymers*, 2022, **14**, 4036.
55 K. Chen, Y. Li, Y. Li, W. Pan and G. Tan, Silk fibroin combined with electrospinning as a promising strategy for tissue regeneration, *Macromol. Biosci.*, 2023, **23**(2), 2200380.
56 S. Prete, M. Dattilo, F. Patitucci, G. Pezzi, O. I. Parisi and F. Puoci, Natural and Synthetic Polymeric Biomaterials for Application in Wound Management, *J. Funct. Biomater.*, 2023, **14**, 455.
57 S. Parham, A. Z. Kharazi, H. R. Bakhsheshi-Rad, M. Kharaziha, A. F. Ismail, S. Sharif, M. Razzaghi, S. RamaKrishna and F. Berto, Antimicrobial synthetic and natural polymeric nanofibers as wound dressing: a review, *Adv. Eng. Mater.*, 2024, **24**(6), 2101460.
58 W. E. Teo and S. Ramakrishna, A review on electrospinning design and nanofibre assemblies, *Nanotechnology*, 2006, **17**(14), R89.
59 N. Ashammakhi, I. Wimpenny, L. Nikkola and Y. Yang, Electrospinning: methods and development of biodegradable nanofibres for drug release, *J. Biomed. Nanotechnol.*, 2009, **5**(1), 1–19.
60 A. K. Elyaderani, M. d. C. De Lama-Odría, L. J. d. Valle and J. Puiggalí, Multifunctional Scaffolds Based on Emulsion and Coaxial Electrospinning Incorporation of Hydroxyapatite for Bone Tissue Regeneration, *Int. J. Mol. Sci.*, 2022, **23**, 15016.
61 C. Ammar, Y. El Ghoul and A. El Achari, Finishing of polypropylene fibers with cyclodextrins and polyacrylic acid as a crosslinking agent, *Text. Res. J.*, 2015, **85**(2), 171–179.
62 Y. El Ghoul, F. Salah, H. Majdoub and F. Sakli, Synthesis and study of drug delivery system obtained via β-cyclodextrin functionalization of viscose/polyester dressings, *J. Ind. Text.*, 2017, **47**(4), 489–504.
63 Y. El Ghoul, R. Renia, I. Faye, S. Rassou, N. Badi, V. Bennevault-Celton, C. Huin and P. Guégan, Biomimetic artificial ion channels based on beta-cyclodextrin, *Chem. Commun.*, 2013, **49**(99), 11647–11649.
64 F. Salah, Y. El Ghoul and S. Roudesli, Bacteriological effects of functionalized cotton dressings, *J. Text. Inst.*, 2016, **107**(2), 171–181.
65 F. M. Alminderej, C. Ammar and Y. El-Ghoul, Functionalization, characterization and microbiological performance of new biocompatible cellulosic dressing grafted chitosan and Suaeda fruticosa polysaccharide extract, *Cellulose*, 2021, **28**, 9821–9835.
66 Y. El-Ghoul and F. M. Alminderej, Bioactive and superabsorbent cellulosic dressing grafted alginate and Carthamus tinctorius polysaccharide extract for the treatment of chronic wounds, *Text. Res. J.*, 2021, **91**(3–4), 235–248.
67 Y. El-Ghoul, Biological and microbiological performance of new polymer-based chitosan and synthesized amino-cyclodextrin finished polypropylene abdominal wall prosthesis biomaterial, *Text. Res. J.*, 2020, **90**(23–24), 2690–2702.
68 M. Keshvardoostchokami, S. S. Majidi, P. Huo, R. Ramachandran, M. Chen and B. Liu, Electrospun Nanofibers of Natural and Synthetic Polymers as Artificial Extracellular Matrix for Tissue Engineering, *Nanomaterials*, 2021, **11**, 21.
69 A. D. J. Bombin, N. J. Dunne and H. O. McCarthy, Electrospinning of natural polymers for the production of nanofibres for wound healing applications, *Mater. Sci. Eng. C*, 2020, **114**, 110994.
70 C. Liu, G. Du, Q. Guo, R. Li, C. Li and H. He, Fabrication and Characterization of Polylactic Acid Electrospun Wound Dressing Modified with Polyethylene Glycol, Rosmarinic Acid and Graphite Oxide, *Nanomaterials*, 2023, **13**, 2000.
71 Y. Ding, W. Li, F. Zhang, Z. Liu, N. Zanjanizadeh Ezazi, D. Liu and H. A. Santos, Electrospun fibrous architectures for drug delivery, tissue engineering and cancer therapy, *Adv. Funct. Mater.*, 2019, **29**(2), 1802852.

72 M. Abrigo, S. L. McArthur and P. Kingshott, Electrospun nanofibers as dressings for chronic wound care: advances, challenges, and future prospects, *Macromol. Biosci.*, 2014, **14**(6), 772–792.
73 Y. L. Tai, L. C. Chen and T. L. Shen, Emerging Roles of Focal Adhesion Kinase in Cancer, *BioMed Res. Int.*, 2015, **2015**, 1–13.
74 T. Okegawa, R. C. Pong, Y. Li and J. T. Hsieh, The role of cell adhesion molecule in cancer progression and its application in cancer therapy, *Acta Biochim. Pol.*, 2004, **51**, 445–457.
75 A. Dbeibia, F. B. Taheur, K. A. Altammar, N. Haddaji, A. Mahdhi, Z. Amri, R. Mzoughi and C. Jabeur, Control of Staphylococcus aureus methicillin resistant isolated from auricular infections using aqueous and methanolic extracts of Ephedra alata, *Saudi J. Biol. Sci.*, 2022, **29**(2), 1021–1028.
76 S. Shi, Y. Si, Y. Han, T. Wu, M. I. Iqbal, B. Fei, R. K. Li, J. Hu and J. Qu, Recent progress in protective membranes fabricated via electrospinning: Advanced materials, biomimetic structures, and functional applications, *Adv. Mater.*, 2022, **34**, 2107938.
77 X. Xie, Y. Chen, X. Wang, X. Xu, Y. Shen, A. u. R. Khan, A. Aldalbahi, A. E. Fetz, G. L. Bowlin, M. El-Newehy and X. Mo, Electrospinning nanofiber scaffolds for soft and hard tissue regeneration, *J. Mater. Sci. Technol.*, 2020, **59**, 243–261.
78 Z. Mohammadalizadeh, E. Bahremandi-Toloue and S. Karbasi, Recent advances in modification strategies of pre- and postelectrospinning of nanofiber scaffolds in tissue engineering, *React. Funct. Polym.*, 2022, **172**, 105202.
79 M. Zafar, S. Najeeb, Z. Khurshid, M. Vazirzadeh, S. Zohaib, B. Najeeb and F. Sefat, Potential of electrospun nanofibers for biomedical and dental applications, *Materials*, 2016, **9**, 73.
80 C. L. Casper, J. S. Stephens, N. G. Tassi, D. B. Chase and J. F. Rabolt, Controlling surface morphology of electrospun polystyrene fibers: effect of humidity and molecular weight in the electrospinning process, *Macromolecules*, 2003, **37**, 573–578.
81 G. C. Ingavle and J. K. Leach, Advancements in electrospinning of polymeric nanofibrous scaffolds for tissue engineering, *Tissue Eng., Part B*, 2014, **20**, 277–293.
82 N. Bhardwaj and S. C. Kundu, Electrospinning: a fascinating fiber fabrication technique, *Biotechnol. Adv.*, 2010, **28**, 325–347.
83 N. Amariei, L. R. Manea, A. P. Bertea, A. Bertea and A. Popa, The influence of polymer solution on the properties of electrospun 3D nanostructures, *IOP Conf. Ser.: Mater. Sci. Eng.*, 2017, **209**, 012092.
84 W. Bao, Y. Zhang, G. Yin and J. Wu, The structure and property of the electrospinning silk fibroin/gelatin blend nanofibers, *e-Polym.*, 2008, **8**, 098.
85 A. Z. Bazmandeh, E. Mirzaei, M. Fadaie, S. Shirian and Y. Ghasemi, Dual spinneret electrospun nanofibrous/gel structure of chitosan-gelatin/chitosan-hyaluronic acid as a wound dressing: in vitro and in vivo studies, *Int. J. Biol. Macromol.*, 2020, **162**, 359–373.
86 Y. EL-Ghoul, C. Ammar, F. M. Alminderej and M. Shafiquzzaman, Design and Evaluation of a New Natural Multi-Layered Biopolymeric Adsorbent System-Based Chitosan/Cellulosic Nonwoven Material for the Biosorption of Industrial Textile Effluents, *Polymers*, 2021, **13**, 322.
87 M. Jridi, S. Hajji, H. B. Ayed, I. Lassoued, A. Mbarek, M. Kammoun, N. Souissi and M. Nasri, Physical, structural, antioxidant and antimicrobial properties of gelatin–chitosan composite edible films, *Int. J. Biol. Macromol.*, 2014, **67**, 373–379.
88 A. Z. Bazmandeh, E. Mirzaei, M. Fadaie, S. Shirian and Y. Ghasemi, Dual spinneret electrospun nanofibrous/gel structure of chitosan-gelatin/chitosan-hyaluronic acid as a wound dressing: in vitro and in vivo studies, *Int. J. Biol. Macromol.*, 2020, **162**, 359–373.
89 N. Naseri, C. Algan, V. Jacobs, M. John, K. Oksman and A. P. Mathew, Electrospun chitosan-based nanocomposite mats reinforced with chitin nanocrystals for wound dressing, *Carbohydr. Polym.*, 2014, **109**, 7–15.
90 H.-H. Park, S.-C. Ko, G.-W. Oh, S.-J. Heo, D.-H. Kang, S.-Y. Bae and W.-K. Jung, Fabrication and characterization of phlorotannins/poly (vinyl alcohol) hydrogel for wound healing application, *J. Biomater. Sci., Polym. Ed.*, 2018, **29**, 972–983.
91 S. S. Letha, A. S. Kumar, U. Nisha and M. J. Rosemary, Electrospun polyurethane-gelatin artificial skin scaffold for wound healing, *J. Text. Inst.*, 2021, **113**, 1–10.
92 S. Y. Gu, Z. M. Wang, J. Ren and C. Y. Zhang, Electrospinning of gelatin and gelatin/poly(l-lactide) blend and its characteristics for wound dressing, *Mater. Sci. Eng., C*, 2009, **29**, 1822–1828.
93 E. H. Kim, S. Lim, E. Kim, I. O. Jeon and Y. S. Choi, Preparation of in situ injectable chitosan/gelatin hydrogel using an acid-tolerant tyrosinase, *Biotechnol. Bioprocess Eng.*, 2018, **23**, 500–506.
94 P. I. Morgado, A. Aguiar-Ricardo and I. J. Correia, Asymmetric membranes as ideal wound dressings: An overview on production methods, structure, properties and performance relationship, *J. Membr. Sci.*, 2015, **490**, 139–151.
95 R. Khajavi and M. Abbasipour, *Controlling Nanofiber Morphology by the Electrospinning Process*, ed. Afshari, M., Woodhead Publishing, Cambridge, UK, 1st edn, 2017, pp. 109–123.
96 L. Jeong and W. H. Park, Preparation and characterization of gelatin nanofibers containing silver nanoparticles, *Int. J. Mol. Sci.*, 2014, **15**, 6857–6879.
97 M. Okhawilai, R. Rangkupan, S. Kanokpanont and S. Damrongsakkul, Preparation of Thai silk fibroin/gelatin electrospun fiber mats for controlled release applications, *Int. J. Biol. Macromol.*, 2010, **46**, 544–550.
98 M. R. Kasaai, A review of several reported procedures to determine the degree of N-acetylation for chitin and

chitosan using infrared spectroscopy, *Carbohydr. Polym.*, 2008, **71**(4), 497–508.

99 P. Cazón, G. Velázquez and M. Vázquez, Characterization of bacterial cellulose films combined with chitosan and polyvinyl alcohol: Evaluation of mechanical and barrier properties, *Carbohydr. Polym.*, 2019, **216**, 72–85.

100 A. E. Stoica, D. Albuleț, A. C. Bîrcă, F. Iordache, A. Ficai, A. M. Grumezescu, B. Ș. Vasile, E. Andronescu, F. Marinescu and A. M. Holban, Electrospun nanofibrous mesh based on PVA, chitosan, and usnic acid for applications in wound healing, *Int. J. Mol. Sci.*, 2023, **24**(13), 11037.

101 M. F. Alminderej and Y. El-Ghoul, Synthesis and study of a new biopolymer-based chitosan/hematoxylin grafted to cotton wound dressings, *J. Appl. Polym. Sci.*, 2019, **136**, 47625.

102 M. F. Alminderej, Study of new cellulosic dressing with enhanced antibacterial performance grafted with a biopolymer of chitosan and myrrh polysaccharide extract, *Arabian J. Chem.*, 2020, **13**, 3672–3681.

103 C. Ammar, Y. El-Ghoul and M. Jabli, Characterization and valuable use of Calotropis gigantea seedpods as a biosorbent of methylene blue, *Int. J. Phytorem.*, 2021, **23**(10), 1085–1094.

104 S. Selvaraj and N. N. Fathima, Fenugreek incorporated silk fibroin nanofibers a potential antioxidant scaffold for enhanced wound healing, *ACS Appl. Mater. Interfaces*, 2017, **9**, 5916–5926.

105 P. Bhargava, D. Mahanta, A. Kaul, Y. Ishida, K. Terao, R. Wadhwa and S. C. Kaul, Experimental Evidence for Therapeutic Potentials of Propolis, *Nutrients*, 2021, **13**, 2528.

106 A. Kurek-Górecka, M. Kłósek, G. Pietsz, Z. P. Czuba, S. Kolayli, Z. Can, R. Balwierz and P. Olczyk, The Phenolic Profile and Anti-Inflammatory Effect of Ethanolic Extract of Polish Propolis on Activated Human Gingival Fibroblasts-1 Cell Line, *Molecules*, 2023, **28**, 7477.

107 J. R. Dias, P. L. Granja and P. J. Bártolo, Advances in electrospun skin substitutes, *Prog. Mater. Sci.*, 2016, **84**, 314–334.

108 K. Sisson, C. Zhang, M. C. Farach-Carson, D. B. Chase and J. F. Rabolt, Fiber diameters control osteoblastic cell migration and differentiation in electrospun gelatin, *J. Biomed. Mater. Res., Part A*, 2010, **94**, 1312–1320.

109 J. M. Ameer, A. K. PR and N. Kasoju, Strategies to tune electrospun scaffold porosity for effective cell response in tissue engineering, *J. Funct. Biomater.*, 2019, **10**, 30.

110 J. Guo, W. Sun, J. P. Kim, X. Lu, Q. Li, M. Lin, O. Mrowczynski, E. B. Rizk, J. Cheng, G. Qian and J. Yang, Development of tannin-inspired antimicrobial bioadhesives, *Acta Biomater.*, 2018, **72**, 35–44.

111 A. Z. Bazmandeh, E. Mirzaei, M. Fadaie, S. Shirian and Y. Ghasemi, Dual spinneret electrospun nanofibrous/gel structure of chitosan-gelatin/chitosan-hyaluronic acid as a wound dressing: in vitro and in vivo studies, *Int. J. Biol. Macromol.*, 2020, **162**, 359–373.

112 I. Przybyłek and T. M. Karpiński, Antibacterial Properties of Propolis, *Molecules*, 2019, **24**, 2047.

113 N. Nefzi, S. Pagliari, L. Campone, W. Megdiche-Ksouri, F. Giarratana, N. Cicero, G. Ziino and L. Nalbone, Chemical Composition and Comprehensive Antimicrobial Activity of an Ethanolic Extract of Propolis from Tunisia, *Antibiotics*, 2023, **12**, 802.

114 M. A. Matica, F. L. Aachmann, A. Tøndervik, H. Sletta and V. Ostafe, Chitosan as a Wound Dressing Starting Material: Antimicrobial Properties and Mode of Action, *Int. J. Mol. Sci.*, 2019, **20**, 5889.

115 P. Sahariah and M. Másson, Antimicrobial Chitosan and Chitosan Derivatives: A Review of the Structure-Activity Relationship, *Biomacromolecules*, 2017, **18**, 3846–3868.